PHYSICAL REVIEW C **71**, 052801(R) (2005)

The ^{8}Li(d, p)^{9}Li reaction and the astrophysical ^{8}Li(n, γ)^{9}Li reaction rate

Z. H. Li, W. P. Liu, X. X. Bai, B. Guo, G. Lian, S. Q. Yan, B. X. Wang, S. Zeng,
Y. Lu, J. Su, Y. S. Chen, K. S. Wu, and N. C. Shu
China Institute of Atomic Energy, P. O. Box 275(46), Beijing 102 413, P. R. China

T. Kajino
National Astronomical Observatory of Japan, Mitaka, Tokyo 181-8588, Japan;
Department of Astronomy, University of Tokyo, Bunkyo-ku, Tokyo 113-0033 Japan
(Received 12 July 2004; revised manuscript received 28 October 2004; published 19 May 2005)

The ^{8}Li(n, γ)^{9}Li reaction plays an important role in both the r-process nucleosynthesis and the inhomogeneous big bang models. Its direct capture rates can be extracted from the ^{8}Li(d, p)^{9}Li reaction, indirectly. We have measured the angular distribution of the ^{8}Li(d, p)^{9}Li$_{g.s.}$ reaction at $E_{c.m.} = 7.8$ MeV in inverse kinematics using coincidence detection of ^{9}Li and the recoil proton, for the first time. Based on distorted wave Born approximation (DWBA) analysis, the ^{8}Li(d, p)^{9}Li$_{g.s.}$ cross section was determined to be 7.9 ± 2.0 mb. The single particle spectroscopic factor $S_{1,3/2}$ for the ground state of $^9\text{Li} = {}^8\text{Li} \otimes n$ was derived to be 0.68 ± 0.14, and then used to calculate the direct capture cross sections for the ^{8}Li(n, γ)^{9}Li$_{g.s.}$ reaction at energies of astrophysical interest. The astrophysical ^{8}Li(n, γ)^{9}Li$_{g.s.}$ reaction rate for the direct capture was found to be 3970 ± 950 cm^3 mole^{-1} s^{-1} at $T_9 = 1$. This presents the first experimental constraint for the ^{8}Li(n, γ)^{9}Li reaction rates of astrophysical relevance.

DOI: 10.1103/PhysRevC.71.052801 PACS number(s): 25.60.Je, 21.10.Jx, 25.40.Lw, 26.35.+c

The ^{8}Li(n, γ)^{9}Li reaction has attracted much attention in recent years because of its importance in astrophysics. In explosive neutron-rich environments, the stability gap at mass number $A = 8$ can be bridged with reactions involving the unstable nucleus ^{8}Li to synthesize $A > 8$ nuclides. Type II supernovae and inhomogeneous big bang nucleosynthesis are thought to be the astrophysical sites for such nucleosynthetic processes.

In the recently developed scenario of the r-process nucleosynthesis occurring with type II supernovae [1,2], all preexisting nuclei, in the region between the nascent neutron star and the shock front, are believed to have been photodisintegrated to protons and neutrons at the initial high temperature. With the descent of temperature, they recombine mostly under nuclear statistical equilibrium, leading to the production of seed nuclei for the r process. When a high α-particle abundance forms, the main reaction chain is initiated by ^{4}He(αn, γ)^{9}Be(α, n)^{12}C. After α-rich freezeout, however, ^{4}He(t, γ)^{7}Li(n, γ)^{8}Li(α, n)^{11}B becomes one of the active reaction chains to produce seed nuclei. In this phase, the ^{8}Li(n, γ)^{9}Li reaction, which leads to the production of ^{9}Be via the ^{9}Li β decay, is in competition with the ^{8}Li(α, n)^{11}B reaction. The competition determines which reaction path is taken. This reaction also competes with the ^{8}Li β decay. Depending on the rate, ^{8}Li(n, γ)^{9}Li may influence the abundance of seed nuclei to some extent. Recently, binary neutron star mergers have been proposed as possible alternative sites for the r process [3], in which a similar situation is found.

The inhomogeneous big bang models [4] predict relatively higher abundances of $A > 8$ nuclides than the standard model. An unconvincing agreement [5] between observed primordial abundances and those predicted with the standard model may point to the need for inhomogeneous models, in which ^{7}Li(n, γ)^{8}Li(α, n)^{11}B are generally thought to be the major reaction chains forming heavier nuclei. However, it has been found that ^{7}Li(n, γ)^{8}Li(n, γ)^{9}Li(α, n)^{12}B may be even more important [6], as the ^{8}Li(n, γ)^{9}Li reaction affects not only the reaction path to $A > 8$ isotopes but also the abundances of Li, Be, B, and C.

Considerable effort has been devoted to experimentally determining the ^{8}Li(α, n)^{11}B cross section as described in Ref. [7] and references therein. However, a large uncertainty still remains for the ^{8}Li(n, γ)^{9}Li cross section. There were some microscopic and systematic calculations of this reaction that deviated by an order of magnitude [6,8–12]. Direct measurement of the ^{8}Li(n, γ)^{9}Li reaction is impossible because no neutron target exists, and the half-life of ^{8}Li is too short (838 ms) as a target. The only experimental information was obtained from two Coulomb dissociation measurements [13,14] that presented the different upper limits. Therefore, measurement of the ^{8}Li(n, γ)^{9}Li cross section through an independent approach is greatly needed. A practicable method is to extract the direct capture cross section for the ^{8}Li(n, γ)^{9}Li reaction using the direct capture model [15,16] and the spectroscopic factor, which can be deduced from the angular distribution of the transfer reaction ^{8}Li(d, p)^{9}Li.

To date, the only measurement of the ^{8}Li(d, p)^{9}Li reaction, performed in the 1990s [17], presented an upper limit of cross section, though no ^{9}Li events were detected. In the present work, we measured the angular distribution of the ^{8}Li(d, p)^{9}Li$_{g.s.}$($Q = 1.839$ MeV) reaction at $E_{c.m.} = 7.8$ MeV in inverse kinematics, and derived the ^{8}Li(n, γ)^{9}Li$_{g.s.}$ direct capture cross sections at energies of astrophysical interest.

The experiment was carried out using the secondary beam facility GIRAFFE [18] of the HI-13 tandem accelerator in Beijing. A 44-MeV ^{7}Li primary beam from the tandem impinged on a 4.8-cm deuterium gas cell at a pressure of 1.6 atm. The front and rear windows of the gas cell were Havar

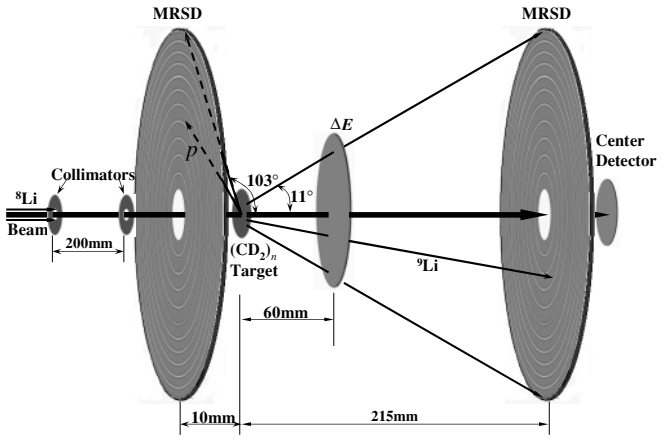

FIG. 1. Schematic layout of the experimental setup.

foils, each with a thickness of 1.9 mg/cm^2. The ^{8}Li ions were produced via the ^{2}H(^{7}Li, ^{8}Li)^{1}H reaction. After the magnetic separation and focus with a dipole and a quadrupole doublet, the 39-MeV ^{8}Li secondary beam was delivered. Typical purity of the ^{8}Li beam was about 80%; the main contaminants were ^{7}Li ions from Rutherford scattering of the primary beam in the gas cell windows and the beam tube. The ^{8}Li beam was then collimated with two apertures of diameter 3 mm and directed onto a $(CD_2)_n$ target with a thickness of 1.5 mg/cm^2 to study the ^{2}H(^{8}Li, ^{9}Li)^{1}H reaction; the typical beam intensity on the target was approximately 1000 pps. The beam energy spread on the target was 0.52 MeV full width half maximum (FWHM) for long-term measurement, and the beam angular divergence was about $\pm 0.3^\circ$. A carbon target with a thickness of 1.8 mg/cm^2 served as the background measurement.

The experimental setup is shown in Fig. 1. Two 300-μm thick multiring semiconductor detectors (MRSDs) with center holes were used. The upstream one was aimed at detection of the recoil protons, and the downstream one, backed by an independent 300-μm thick silicon detector placed at the center hole, served as a residue energy (E_r) detector which formed a $\Delta E - E_r$ counter telescope together with a 21.7-μm thick silicon ΔE detector. Such a detector configuration covered the laboratory angular ranges of 0 to 11° (greater than the maximum $\theta_{\rm lab}$ of ^{9}Li, 10.7°) and 103 to 170°, respectively. For coincidence measurement, the detectable angular range of ^{9}Li in the center of mass system was from 10 to 50°. This setup also facilitated precise determination of the accumulated quantity of incident ^{8}Li because the ^{8}Li themselves were recorded by the counter telescope simultaneously.

The accumulated quantity of incident ^{8}Li for the $(CD_2)_n$ target measurement was approximately 1.66×10^8, and 1.11×10^7 for measurement with the carbon target. Figure 2 displays the summing $\Delta E - E_r$ scatter plot of the coincidence events over all the rings of the downstream MRSD. In order to scrutinize the origin of non-^{9}Li region events in Fig. 2, four typical regions were selected in which the ratios of events in the coincidence spectrum to those in the non-coincidence one were compared. It was found that the ratio in the ^{9}Li region is much higher than those (nearly constant) in the other three regions. We can thus conclude that the events in non-^{9}Li regions result from the random coincidence caused by the

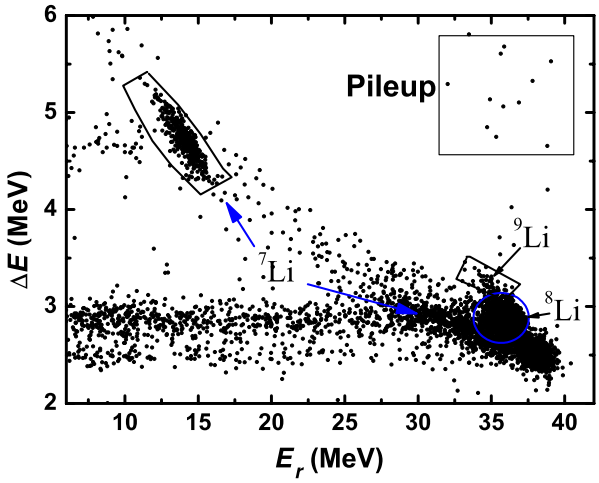

FIG. 2. (Color online) Scatter plot of ΔE vs. E_r for the ^{9}Li-proton coincidence measurement with a $(CD_2)_n$ target. The four regions were selected to scrutinize the random coincidence events.

noise tail in the proton spectrum of the upstream MRSD. The scatter plot of E_t vs. $\theta_{\rm lab}$ for the events within the ^{9}Li gate in Fig. 2 is shown in Fig. 3. The zone between the two solid lines represents the kinematics region of the ^{9}Li ground state, based on a Monte Carlo simulation. Figure 3 further demonstrates that the events within the ^{9}Li gate in Fig. 2 are the true ^{9}Li products. Actually, the selection of ^{9}Li events was individually performed for each ring of the downstream MRSD. The energies and angles of protons on the upstream MRSD relevant to the ^{9}Li events appearing on a specific ring of the downstream MRSD were restricted with the kinematics. Thus, the random coincidence events were effectively depressed by setting the corresponding windows for energies and angles (ring numbers) of protons. Finally, about 50 ^{9}Li events were identified for the measurement with the $(CD_2)_n$ target, and no background event was found in the same region for the carbon target run.

Because of the existence of dead gaps in both MRSDs, a Monte Carlo simulation was used to calculate the coincidence

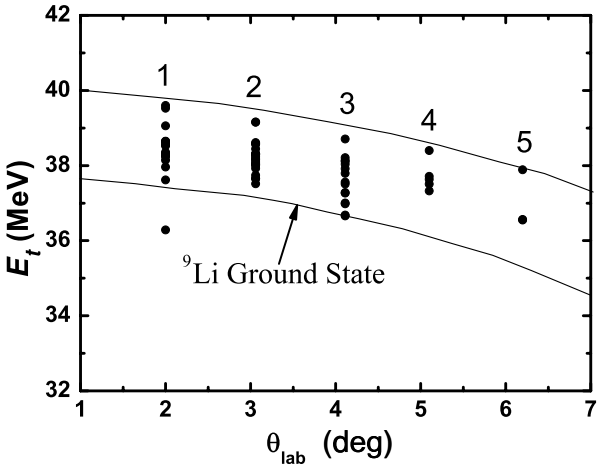

FIG. 3. Scatter plot of E_t vs. $\theta_{\rm lab}$ for the events within the ^{9}Li gate in Fig. 2. The ring numbers of the downstream MRSD are indicated.

efficiency between ^{9}Li ions detected by the downstream MRSD and protons detected by the upstream one. The simulation took the geometrical factor, angular straggling, and energy straggling into account. The coincidence efficiency was deduced from the ratio of the proton events in the relevant rings of the upstream MRSD to the ^{9}Li events in a specific ring of the downstream one. The differential cross sections can then be deduced. The resultant angular distribution is shown in Fig. 4. The uncertainties of differential cross sections mainly arise from the statistics and the assignment of the ^{9}Li gate; the angular uncertainties are from the angular divergence of the ^{8}Li beam, the finite size of the beam spot, the angular straggling in the target and ΔE detector, as well as the width of each ring of the downstream MRSD.

The spin and parity of the ^{8}Li and ^{9}Li (ground state) are 2^+ and $3/2^-$, respectively. The ^{8}Li$(d, p)^9$Li$_{\text{g.s.}}$ cross section involves two components corresponding to $(l = 1, j = 3/2)$ and $(l = 1, j = 1/2)$ transfers. The differential cross section can be expressed as

$$\left(\frac{d\sigma}{d\Omega}\right)_{\text{exp}} = S_d[S_{1,3/2}\sigma_{1,3/2}(\theta) + S_{1,1/2}\sigma_{1,1/2}(\theta)], \qquad (1)$$

where $(\frac{d\sigma}{d\Omega})_{\text{exp}}$ and $\sigma_{l,j}(\theta)$ denote the measured and distorted wave Born approximation (DWBA) differential cross sections, respectively; $S_{1,3/2}$ and $S_{1,1/2}$ are spectroscopic factors for the ground state of ^{9}Li $=^8$Li $\otimes\, n$, corresponding to the $j = 3/2$ and $1/2$ orbits. S_d is the spectroscopic factor of deuteron that is close to unity. The $S_{1,3/2}$ and $S_{1,1/2}$ can be extracted by normalizing DWBA differential cross sections to the experimental data.

The finite-range DWBA code PTOLEMY [19] was used to compute the angular distribution. In the calculation, only the neutron transfer to the $1p3/2$ orbit was taken into account because the contribution of the $1p1/2$ orbit is less than 5% [16,20]. All the entrance channel parameters were taken from Ref. [21]; the exit channel parameters were taken from Refs. [21] and [22], respectively. Figure 4 presents the normalized angular distributions for four sets of optical potential parameters, each curve corresponding to one spectroscopic factor $S_{1,3/2}$. The average value of these spectroscopic factors was found to be 0.68 ± 0.14 with the "standard" bound state potential parameters (radius $r_0 = 1.25$ fm, diffuseness $a = 0.65$ fm), which agrees fairly well with the result $S_{1,3/2} = 0.73$ extracted from the mirror reaction ^{8}B$(d, n)^9$C [20]. The cross section for the ^{8}Li$(d, p)^9$Li$_{\text{g.s.}}$ reaction at $E_{\text{c.m.}} = 7.8$ MeV was determined to be 7.9 ± 2.0 mb through integration of the calculated angular distributions. The uncertainties of the spectroscopic factor and cross section result mainly from the difference of the optical potentials used in the calculation, as well as the statistical error of the measurement.

The ^{8}Li$(n, \gamma)^9$Li$_{\text{g.s.}}$ cross section was calculated by assuming that the reaction proceeds by direct $E1$ capture of the neutron to the ground state of ^{9}Li. At low energies of astrophysical interest, the contribution of the d wave is negligible, and the capture reaction is almost totally determined by the s wave neutron capture process. The cross section for $E1$ capture of the neutron to the ground state of ^{9}Li with the orbital and

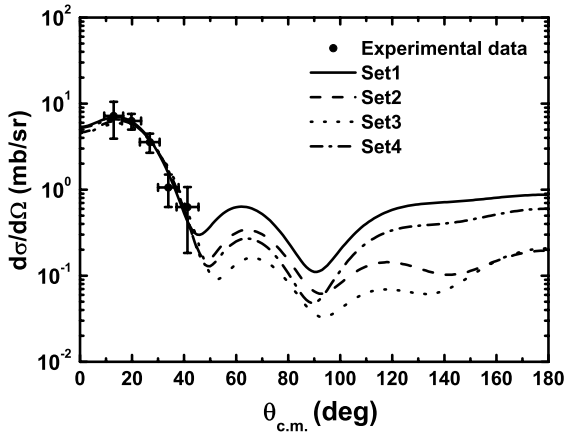

FIG. 4. Measured angular distribution of ^{8}Li$(d, p)^9$Li$_{\text{g.s.}}$ at $E_{\text{c.m.}} = 7.8$ MeV, together with DWBA calculations using various optical potential parameters.

total angular momenta l_f and j_f is given by

$$\sigma_{(n,\gamma)} = \frac{16\pi}{9}\left(\frac{E_\gamma}{\hbar c}\right)^3 \frac{e_{\text{eff}}^2}{k^2}\frac{1}{\hbar v}\frac{(2j_f+1)}{(2I_1+1)(2I_2+1)}S_{l_f j_f} \times \left|\int_0^\infty r^2 w_{l_i}(kr)u_{l_f}(r)dr\right|^2, \qquad (2)$$

where E_γ stands for the γ-ray energy, v is the relative velocity between particles 1 (neutron) and 2 (^{8}Li), k is the incident wave number, and I_i is the spin of particle i. $e_{\text{eff}} = -eZ/(A+1)$ is the neutron effective charge for the $E1$ transition in the potential produced by a target nucleus with mass number A and atomic number Z. $w_{l_i}(kr)$ is the distorted radial wave function for the entrance channel, and $u_{l_f}(r)$ is the radial wave function of the bound state neutron in ^{9}Li which can be calculated by solving the respective Schrödinger equation. The optical potential for the neutron scattering on unstable nucleus ^{8}Li is unknown experimentally. We adopted a real folding potential which was calculated using the ^{8}Li density distribution from the measured interaction cross section [23]

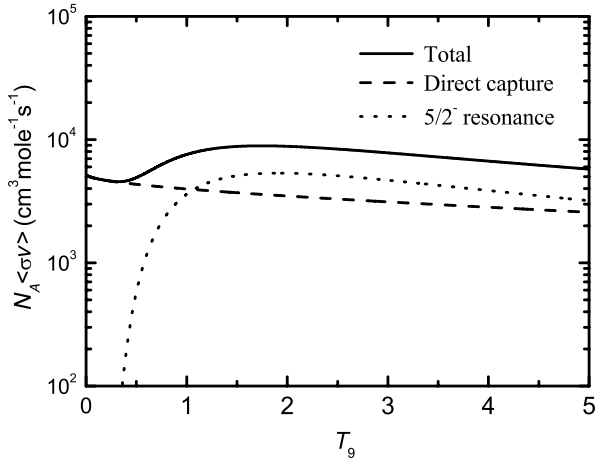

FIG. 5. Temperature dependence of the reaction rates for ^{8}Li$(n, \gamma)^9$Li. The contribution of direct capture is the result of the present work, and that of the $5/2^-$ resonance is taken from Ref. [6].

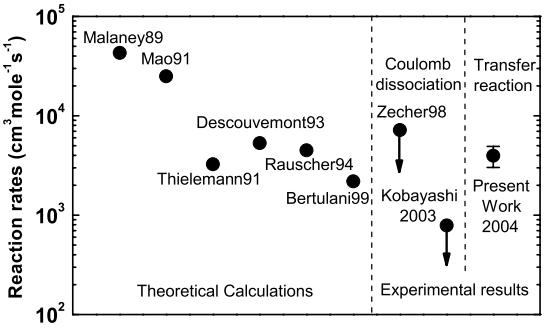

FIG. 6. The ^{8}Li$(n,\gamma)^9$Li reaction rates for the direct capture derived from theoretical calculations and experiments.

and an effective nucleon-nucleon interaction DDM3Y [24]. The imaginary part of the potential is very small because of the small flux into other reaction channels and can be neglected in most cases involving the neutron capture reaction. The depth of the real potential was scaled to $J_V/A = 743$ MeV fm^3, the volume integral of potential per nucleon. Usually, the optical potential changes considerably for different nuclei, whereas the volume integral of potential per nucleon is relatively a more stable quantity. First, we calculated the folding potentials for ^{6,7}Li and ^{12}C, whose neutron capture cross sections were measured [25–27], and we found $J_V/A = 749 \pm 23$, 729 ± 75, and 742 ± 12 MeV fm^3, respectively, by fitting to the experimental cross sections. One can see that these values are close to each other, indicating the stability of the potential volume integral. Then the weighted average of the above values was taken as the J_V/A value for ^{8}Li. As soon as the potential is known, the capture cross sections can be calculated with Eq. (2). With the spectroscopic factor extracted from the present experiment, the energy dependence of direct capture cross section for the ^{8}Li$(n,\gamma)^9$Li$_{\text{g.s.}}$ reaction was calculated, showing a deviation from the usual $1/v$ behavior. Figure 5 demonstrates the temperature dependence of the reaction rate for the direct capture in ^{8}Li$(n,\gamma)^9$Li together with that for the resonant capture at the $5/2^-$ 4.3-MeV state in ^{9}Li (deduced by Rauscher *et al*. [6] with $\Gamma_\gamma = 0.65$ eV and $\Gamma_{\text{tot}} = 100$ keV), as well as the total reaction rate. Direct capture to the first excited state at 2.69 MeV is not included in the calculation since the transition strength is believed to be negligible [13,14]. It can be clearly seen that the direct capture plays an important role in the ^{8}Li$(n,\gamma)^9$Li reaction, especially in the astrophysical environment of $T_9 < 1$. The reaction rate for the direct capture was found to be $N_A\langle\sigma v\rangle = 3970 \pm 950$ cm^3 mole^{-1} s^{-1} at $T_9 = 1$, the uncertainty arising from the errors of spectroscopic factor and the volume integral of potential per nucleon. The ^{8}Li$(n,\gamma)^9$Li reaction rates for the direct capture derived from theoretical calculations and experiments are shown in Fig. 6. Our result is significantly higher than the upper limit from the most recent Coulomb dissociation experiment [13], and approximately in agreement with the theoretical estimations reported in Refs. [6,10].

In summary, we have measured the angular distribution of the ^{8}Li$(d,p)^9$Li$_{\text{g.s.}}$ reaction at $E_{\text{c.m.}} = 7.8$ MeV, through coincidence detection of ^{9}Li and the recoil proton, and obtained the cross section. By using the spectroscopic factor deduced from the ^{8}Li$(d,p)^9$Li$_{\text{g.s.}}$ angular distribution, we have successfully derived the ^{8}Li$(n,\gamma)^9$Li$_{\text{g.s.}}$ direct capture cross section and astrophysical reaction rate for the first time.

This work was supported by the Major State Basic Research Development Program under Grant Nos. G200077400 and 2003CB716704, and the National Natural Science Foundation of China under Grant Nos. 10375096, 10025524, and 19935030.

[1] M. Terasawa, K. Sumiyoshi, T. Kajino, G. J. Mathews, and I. Tanihata, Astrophys. J. **562**, 470 (2001).
[2] T. Kajino, S. Wanajo, and G. J. Mathews, Nucl. Phys. **A704**, 165c (2002).
[3] S. Rosswog, C. Freiburghaus, and F. K. Thielemann, Nucl. Phys. **A688**, 344c (2001).
[4] T. Kajino and R. N. Boyd, Astrophys. J. **359**, 267 (1990).
[5] N. Hata, R. J. Scherrer, G. Steigman, D. Thomas, T. P. Walker, S. Bludman, and P. Langacker, Phys. Rev. Lett. **75**, 3977 (1995).
[6] T. Rauscher, J. H. Applegate, J. J. Cowan, F. K. Thielemann, and M. Wiescher, Astrophys. J. **429**, 499 (1994).
[7] H. Miyatake *et al*., Nucl. Phys. **A738**, 401 (2004).
[8] R. A. Malaney and W. A. Fowler, Astrophys. J. **345**, L5 (1989).
[9] Z. Q. Mao and A. E. Champagne, Nucl. Phys. **A522**, 568 (1991).
[10] F. K. Thielemann, J. H. Cowan, and M. Wiescher, in *Nuclei in the Cosmos*, edited by H. Oberhummer *et al*. (Springer, Berlin, 1991).
[11] P. Descouvemont, Astrophys. J. Lett. **405**, 518 (1993).
[12] C. A. Bertulani, J. Phys. G **25**, 1959 (1999).
[13] H. Kobayashi *et al*., Phys. Rev. C **67**, 015806 (2003).
[14] P. D. Zecher *et al*., Phys. Rev. C **57**, 959 (1998).
[15] C. Rolfs, Nucl. Phys. **A217**, 29 (1973).
[16] P. Mohr, Phys. Rev. C **67**, 065802 (2003).
[17] M. J. Balbes *et al*., Nucl. Phys. **A584**, 315 (1995).
[18] W. Liu *et al*., Nucl. Instrum. Methods Phys. Res. B **204**, 62 (2003).
[19] M. H. Macfarlane and S. C. Pieper, Argonne National Laboratory Report (unpublished).
[20] D. Beaumel, T. Kubo, T. Teranishi, H. Sakurai, S. Fortier, A. Mengoni, N. Aoi, N. Fukuda, M. Hirai, N. Ima, *et al*., Phys. Lett. **B514**, 226 (2001).
[21] C. M. Perey and F. G. Perey, At. Data Nucl. Data Tables **17**, 1 (1976).
[22] B. A. Watson, P. P. Singh, and R. E. Segel, Phys. Rev. **182**, 977 (1969).
[23] I. Tanihata, H. Hamagaki, O. Hashimoto, Y. Shida, N. Yoshikawa, K. Sugimoto, O. Yamakawa, T. Kobayashi, and N. Takahashi, Phys. Rev. Lett. **55**, 2676 (1985).
[24] A. M. Kobos, B. A. Brown, R. Lindsay, and G. R. Satchler, Nucl. Phys. **A425**, 205 (1984).

[25] T. Ohsaki, Y. Nagai, M. Igashira, T. Shima, H. Kitazawa, K. Takaoka, M. Kinoshita, Y. Nobuhara, A. Tomyo, H. Makii *et al*., AIP Conf. Proc. **529(1)**, 458 (2000).

[26] J. C. Blackmon, A. E. Champagne, J. K. Dickens, J. A. Harvey, M. A. Hofstee, S. Kopecky, D. C. Larson, D. C. Powell, S. Raman, and M. S. Smith, Phys. Rev. C **54**, 383 (1996).

[27] Y. Nagai, M. Igashira, N. Mukai, T. Ohsaki, F. Uesawa, K. Takeda, T. Ando, H. Kitazawa, S. Kubono, and T. Fukuda, Astrophys. J. **381**, 444 (1991).